Carbohydrate Polymers 103 (2014) 38–45

Contents lists available at ScienceDirect

Carbohydrate Polymers

journal homepage: www.elsevier.com/locate/carbpol

Electrodeposition of alginate/chitosan layer-by-layer composite coatings on titanium substrates

Zhiliang Wang[a], Xueqin Zhang[a], Juming Gu[b], Haitao Yang[a], Jun Nie[a], Guiping Ma[a,*]

[a] Key Laboratory of Carbon Fiber and Functional Polymers, Ministry of Education, State Key Laboratory of Chemical Resource Engineering, Beijing University of Chemical Technology, Beijing 100029, PR China
[b] Institute of Scientific and Technical Information of China, Beijing 100038, PR China

ARTICLE INFO

Article history:
Received 8 October 2013
Received in revised form 1 November 2013
Accepted 3 December 2013
Available online 12 December 2013

Keywords:
Electrodeposition
Chitosan
Alginate
Layer-by-layer

ABSTRACT

In this study, alginate/chitosan layer-by-layer composite coatings were prepared on titanium substrates via electrodeposition. The mechanism of anodic deposition of anionic alginate based on the pH decrease at the anode surface, while the pH increase at the cathode surface enabled the deposition of cationic chitosan coatings. The surface of coatings was characterized by using attenuated total reflection–Fourier transform infrared spectroscopy (ATR–FTIR), X-ray photoelectron spectroscopy (XPS), and scanning electron microscopy (SEM). The properties of coatings were characterized by X-ray diffraction (XRD) and differential thermal analysis (DTA). Indirect in vitro cytotoxicity test showed that the extracts of coating had no significant effects on cell viability. Moreover, in vitro cytocompatibility test exhibited cell population and spreading tendency, suggesting that the coatings were non-toxic to L929 cells. However, the results revealed that alginate coating was more benefit for cells growing than chitosan coating. The results indicated that the proposed method could be used to fabricate alginate/chitosan layer-by-layer composite coatings on the titanium surface at room temperature and such composite coatings might have potential applications in tissue engineering scaffolds field.

1. Introduction

Electrodeposition, a versatile and efficient approach for fabricating thin and thick films, coatings and free-standing bodies, is an area of increasing interest (Boccaccini, Keim, Ma, Li, & Zhitomirsky, 2010). It is a process in which an imposed electric field is employed to direct charged particles dispersed in a liquid towards an electrode for the assembly of thin films. Compared with other methods of preparing coatings, such as solution casting (López-Lacomba et al., 2006), silane reactions (Bumgardner et al., 2003), and layer-by-layer technique (Cai, Rechtenbach, Hao, Bossert, & Jandt, 2005), electrodeposition has advantages of short processing time, the possibility of room temperature processing, and no require for cross-link agents. The coatings or films prepared with the method of electrodeposition have been widely used in the biomedical and biotechnology fields. Roether et al. applied, for the first time, electrodeposition to coat three-dimensional porous biodegradable polymer (polylactic acid) substates with bioglass particles for bone tissue engineering (Roether et al., 2002). Zhitomirsky, Roether, Boccaccini, and Zhitomirsky (2009) have developed bioactive glass/polymer composite coatings with or without HA nanoparticle inclusions for biomedical applications via electrodeposition. Related work has been investigated electrodeposition of chitosan with paired sidewall electrodes (Cheng et al., 2010). More recently, Gray et al. (2012) reported an anodic method to deposit hydrogel films of the aminopolysaccharide chitosan. The mechanisms of electrodeposition have been investigated and there were only a few known mechanisms for polymer electrodeposition, including electro-polymerization mechanism (Glenis, Horowitz, Tourillon, & Garnier,1984), neutralization mechanism and Ca^{2+}-alginate deposition mechanism (Cheng et al., 2011). For example, neutralization mechanisms (Fernandes et al., 2003; Luo, Xu, Du, & Chen, 2004) could be used to explain electrodeposition of pH-responsive film-forming biopolymers. These mechanisms for biopolymer eletrodeposition relied on the use of an electrical signal to trigger a reversible sol–gel transition.

Chitosan is a cationic natural polymer that carries positive charges with a molecular structure of (1 and 4)-linked 2-amino-2- deoxy-β-D-glucan. Aminopolysaccharide chitosan has been electrodeposited by a cathodic neutralization mechanism (Redepenning, Venkataraman, Chen, & Stafford, 2003). In the process of electrodeposition, the pH of solution near the cathode would increase, which were connected with the electrochemically generated concentration gradient of reactant OH^- ions. When

* Corresponding author. Tel.: +86 1064421310; fax: +86 1064421310.
E-mail address: magp@mail.buct.edu.cn (G. Ma).

0144-8617/$ – see front matter © 2013 Elsevier Ltd. All rights reserved.
http://dx.doi.org/10.1016/j.carbpol.2013.12.007

the pH was above its p*K*a value (~6.3), chitosan solution could, under given condition, undergo a sol–gel transition. The subsequent neutralization of the NH_3^+ groups of chitosan chains in solution near the cathode impeled chitosan to deposite on the electrode.

Alginate is a kind of unbranched polysaccharides consisting of (1 → 4) linked β-D-ManA(M) and α-L-GulA(G) residues at different proportions and with different sequential occurrence. To our knowledge, an alginate solution could form a homogeneous gel at pH below p*K*a. These gels were presumably stabilized by intermolecular hydrogen bonds. The anodic deposition of the acidic polysaccharide alginic acid also was attracting attention because it offered broad opportunities for a diverse range of application. Also the neutralization mechanism allowed for electrodeposition of alginate. Sodium alginate with carboxylate groups ($-COO^-$) "recognized" the local low pH at the anode and "responded" by undergoing protonation (to form –COOH) and precipitation (or gelation) at the anode surface.

In this study, we hypothesized that chitosan and alginate could be deposited onto the titanium electrodes layer-by-layer via electrodeposition. Scheme 1 showed that the electrodes were first contacted with neutral sodium alginate and then acidic chitosan solution, respectively. As expected, two thin layers were deposited on the surface of the titanium electrode. The material deposited was chitosan and alginate multilayer composite films, which were tested by SEM, XRD, XPS and ATR–FTIR.

2. Experimental

2.1. Materials.

Chitosan (Mw 100,000, degree of deacetylation (DDA) 87%) and sodium alginate (SA, 1.28 Pa s for a 2 wt% aqueous solution at 30 °C) were purchased from Zhejiang Golden-Shell Biochemical Co., Ltd. (Zhejiang, China) and Sinopharm Chemical Reagent Co., Ltd. (Shanghai, China), respectively. Commercial pure titanium was supplied by Shanxi baoji new metal materials co., LTD. Other reagents and solvents were of analytic grade and purchased from Beijing Chemical Reagent Company. Ultrapure water with specific resistance around 18.25 MΩ cm was used to prepare the solution.

2.2. Titanium substrates preparation

Titanium pieces were cut into rectangular plates (6 × 2 × 0.25 cm) as electrode. All the plates were polished with raw emery paper and fine sandpaper in sequence. Then, the polished plates were chemical polished with mixed acid solution (nitric acid: hydrofluoric acid: water volume ratio 4:1:5). After that, they were ultrasonically cleaned with acetone, ethanol, and ultrapure water for 30 min each then rinsed with ultrapure water.

2.3. Eletrodeposited process

The thickness of the deposited layer was observed to be dependent upon the deposition time, the applied voltage, and the concentration of chitosan and sodium alginate. Chitosan and sodium alginate solution were obtained by dissolving 75 mg of each material in 100 mL of deionized water and 100 mL of 1% (V/V) acetic acid, respectively. All the stock solutions were stirred with magnet for about 30 min. The pH of sodium alginate and chitosan solution was 2.8 and 7.4, respectively. During electrodeposited process, Ti plate was used as anode to deposite first layer alginate and parallel platinum plate as counterelectrode. After dried, depositing of second layer chitosan, the above Ti plate was used as cathode and parallel platinum plate as counterelectrode, then repeated for several times. The electrolyzer cell was cuboid-shaped (5.5 × 3 × 2 cm). Deposition was performed by connecting both the cathode and the anode to a direct current power supply (Model 1719A-5, Dahua electronic) with a constant voltage of 20 V for 20 min. After deposition, the electrodes were rinsed with ultrapure water, and finally dried at 50 °C in the oven overnight.

2.4. Characterization

The surface chemistry of the coatings was investigated by attenuated total reflection Fourier transform infrared spectroscopy (ATR–FTIR; Nicolet Spectra 5700 spectrometer, Nicolet Instrument, Thermo Company, Madison, USA). X-ray diffraction pattern (XRD) of the coatings was identified by using a Rigaku D/Max2500VB2+/Pc diffractometer (Rigaku Company, Tokyo, Japan) with 40 kV and 50 mA with Cu *K*α radiation (λ = 0.154 nm). The scanning scope of 2θ was 5–50° and the scanning rate was 5°/min. Surface morphology of the coatings was observed by scanning electron microscopy by using a Hitachi S-4700 microscope with sputter coated of gold before observation. Thermogravimetric analysis was performed on TGA Q500 (TA Instruments). Each membrane sample in an aluminum copple with the same weight (about 6 mg) was run from room temperature to 800 °C at a scanning rate of 10 °C/min under a nitrogen atmosphere. X-ray photoelectron spectroscopy (XPS) spectra were obtained by using a VG ESCALAB MKII X-ray photoelectron spectrometer (VG Scientific Ltd., UK) with Al *K*α radiation. Survey spectra were recorded for 0–1350 eV binding energy range.

2.5. Swelling properties study

Swelling behavior of the electrodeposited chitosan coating, alginate coating and alginate/chitosan coatings (1 mm × 1 mm) were determined by equilibrium swelling studies, according to a recently procedure (Yang et al., 2010). At room temperature, each coating was immersed in 100 mL PBS buffer solution, respectively. The swollen coatings were processed with filter paper to remove adsorbed water on the surface of coatings. The swelling percentage was calculated from the following equation:

$$E_{sw} = \left[\frac{(w_t - w_o)}{w_o}\right] \times 100$$

where w_t is the weight of the sample at the time t, and w_o is the initial weight of the sample. In order to make the experiments more accurate, experiments had been repeated for three times.

2.6. In vitro cell cytotoxicity

In vitro cytotoxicity of the extracts and cytocompatibility of the alginate/chitosan coatings and alginate/chitosan/alginate coatings were assessed by using mouse L929 fibroblasts cells line.

2.6.1. Indirect cytotoxicity assay

Mouse L929 fibroblast cells were cultured in 200 μL DMEM (Dullecco's modified Eagle's medium; Sigma–Aldrich, USA) medium with 10% FBS (fetal bovine serum), together with 1.0% penicillin-streptomycin and 1.2% glutamine at 37 °C under a wet atmosphere containing 5% CO_2. When cells reached 80–90% confluence, they were trypsinized with 0.25% trypsin containing 1 mL Ethylene Diamine Tetraacetie Acid (EDTA) and suspended in the culture medium. For the MTT assay, the coatings were previously sterilized by high temperature in a hermetically-sealed instrument and then placed in 24-well tissue culture plates under aseptic condition. The samples were then incubated in 1 mL of DMEM at 37 °C for 24 h. After that, the coatings were removed and the extracts were obtained and further diluted to get extraction medium samples. Mouse fibroblasts cells were seeded in wells of a 96-well plate at a density of 4000 cells per well. After incubation for

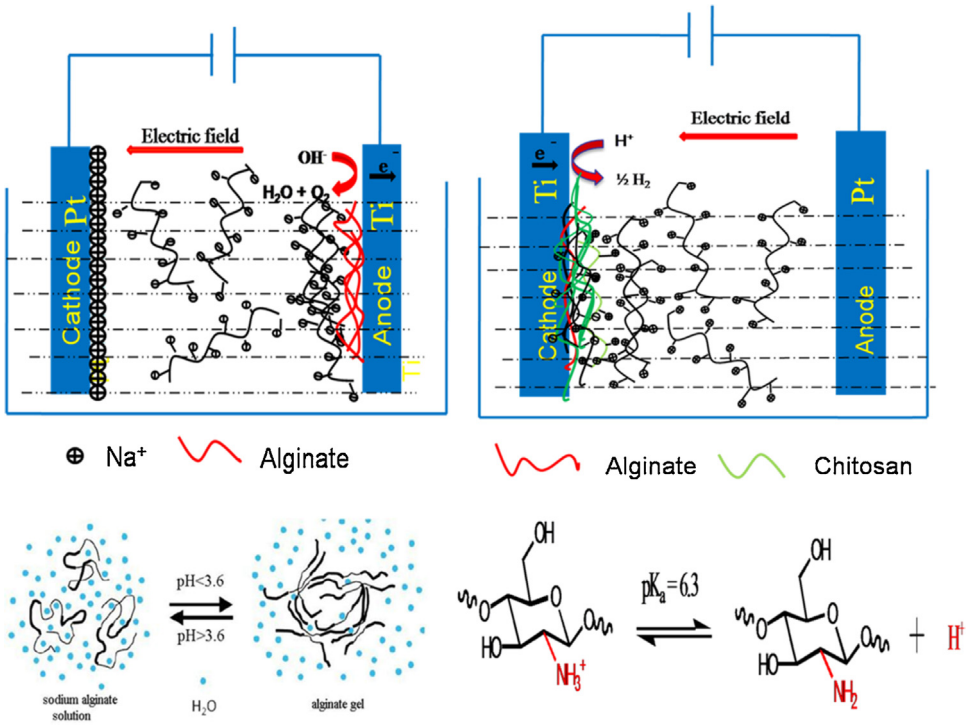

Scheme 1. The diagram of experimental process.

another 24 h, the culture medium was removed and replaced with the extraction medium and incubated for 24 h. The viability of cells was determined by the MTT ((3-[4,-dimethylthiazol-2-yl]-2,5-diphenyltetrazolium bromide; thiazolyl blue) assay (Yin, Yao, Cheng, & Ma, 1999) and about 100 μL of MTT solution was added to each well. After 24 hours incubation at 37 °C, 200 μL of dimethyl sulfoxide was added to dissolve the formazan crystals. The optical density of the formazan solution was detected by an ELISA reader (Multiscan MK3, Labsystem Co.Finland) at 490 nm. For reference purposes, cells were seeded to medium containing 0.64% phenol (positive control) and a fresh culture medium (negative control) under the same seeding conditions, respectively.

2.6.2. In vitro cytocompatibility assay

The cytocompatibility of the coatings was evaluated by directly seeding L929 cells onto the test samples in vitro, and the results were observed by fluorescence microscopy and Scanning Electron Microscopy.

For fluorescence microscopy observation, the prepared square samples (1 cm × 1 cm) were first soaked into the 250 mL phosphate buffer solution (PBS pH = 7.4) for 24 h before sterilization with highly compressed steam for 15 min, then the samples were transferred to the 24-well tissue culture plate. 1 mL of Fibroblasts cells suspension with 1.5×10^4 cells/mL was seeded on the samples. After 48 h of culture, collected cellular was rinsed twice with phosphate buffer solution (PBS) to remove non-adherent cells, subsequently fixed by 75% alcohol solution, observed by fluorescence microscope.

For SEM analysis, the coatings were first fixed on the glass slide. The sample was sterilized, rinsed three times with sterile phosphate buffer solution (PBS), then transferred to individual 24-well tissue culture plates. Aliquots (1 mL) of Fibroblasts cells suspension with 1.5 × 104 cells/mL were seeded on the sample membranes. After 24 h of culture, cellular constructs were harvested and rinsed twice with PBS to remove non-adherent cells. Then they were fixed with 2.5% glutaraldehyde solution. After being thoroughly washed with PBS, the samples were dehydrated through a serious of graded ethanol and dried over night at room temperature. The dried samples were coated with gold by sputtering for further cell morphology analysis on the surface of the coatings by SEM.

3. Results and discussion

3.1. Topography description

Structure of the coatings was shown in Fig. 1. The images presented that the alginate coating had macroporous structure (Fig. 1a). The pore size ranged from 50 to 250 μm, which was connected with the generation of O_2 gas on titanium surface during anodic polarization. During the electrodeposition process, the pH of solution near anode and cathode were 3.2 and 12.5, respectively. The pH of anode solution made alginate solution undergo a sol–gel transition and deposited on the titanium surface. The composite coatings of alginate/chitosan and alginate/chitosan/alginate were shown in Fig. 1b and c, respectively. In order to illustrate different layers depositing on the titanium substrates more visualized, the SEM fracture surface of coatings were provided in Fig. 1d and e. As shown in Fig. 1d, the thickness of alginate and chitosan coatings were about 10 μm and 20 μm, respectively. The reason why the chitosan layer was thicker than the alginate layer was that the molecular weight of chitosan was higher than alginate and abundant hydroxyl and amino groups existed in the molecular chain, the entanglement between the chitosan molecules was much easier in the process of electrodeposition and much more chitosan molecules migrated to the electrode in the same condition. Between two layers, chitosan and alginate could form polyelectrolyte complexes, resulting from electrostatic interaction between NH_3^+ of chitosan and COO^- of alginate. As shown in Fig. 1e, both sides of the composite coatings were alginate and the Sandwich layer was chitosan coating. The maximum electrodeposition layers

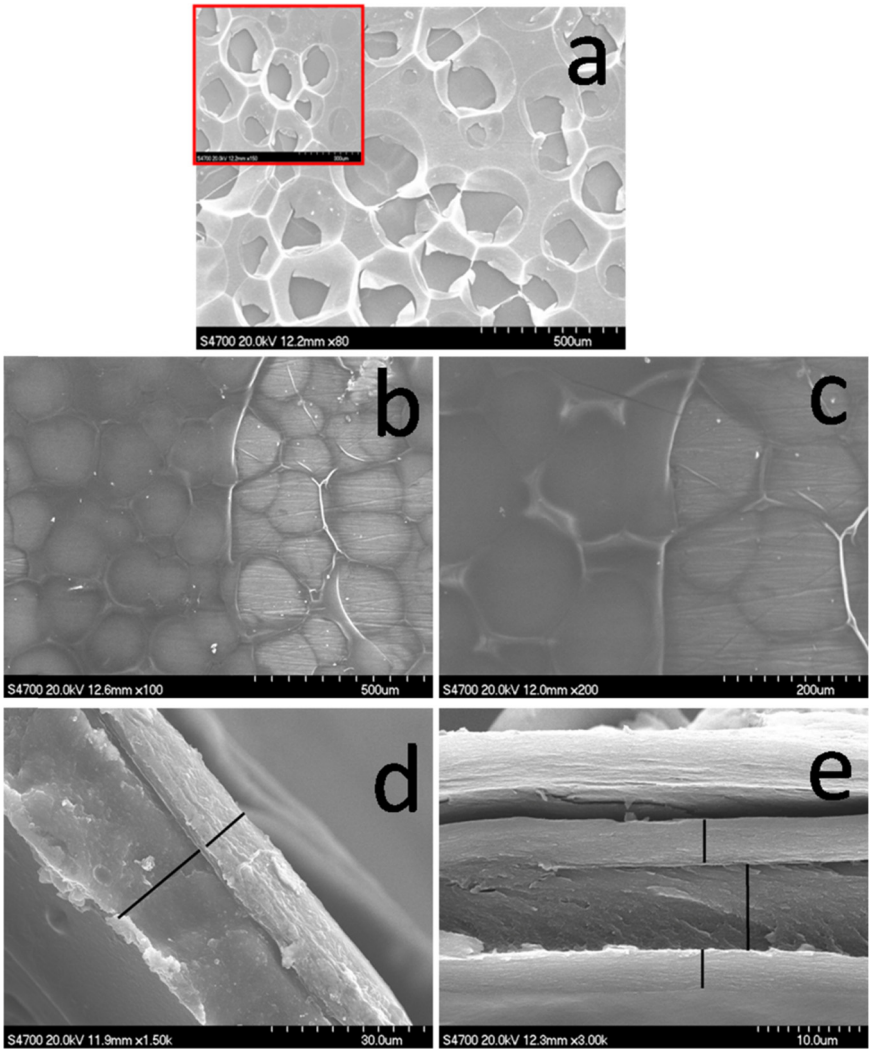

Fig. 1. SEM micrographs of pure alginate and alginate/chitosan coatings: (a) pure alginate coating; (b) alginate/chitosan coatings; (c) alginate/chitosan/alginate coatings; (d) fracture surface of alginate/chitosan coatings; (e) fracture surface of alginate/chitosan/alginate coating.

were four, two alginate layers and two chitosan layers. The layers were too thick to electric, and the electrolysis of water could not happen, resulting in invariability of the pH of solution near the electrode and alginate or chitosan losing the ability of deposition. When alginate was the outermost layer (Fig. 1a), the amine groups of chitosan coating would be protonated to a larger degree due to interaction with deprotonated carboxylate groups of alginate. However, when chitosan was the outermost layer (Fig. 1b), the amine groups extending into solution during fabrication would become deprotonated (Lawrie et al., 2007). Repeating the experiment we conducted above, the composite coatings with multilayers could be achieved.

3.2. ATR–FTIR analysis

In order to illustrate the surface structure or composition of the composite coatings more clearly, ATR–FTIR was used, as showed in Fig. 2. The spectrum of the alginate coating coated on titanium substrate displayed strong peaks at 1723, 1084, and 1035 cm^{-1} (Fig. 2a), which were characteristic peaks of a polysaccharide structure due to –COOH stretching, C–O stretching, and C–O–C stretching (Sartori, Finch, Ralph, & Gilding, 1997). This indicated that Na-alginate solution could, under electrodeposited process, undergo a sol–gel transition and carboxylate groups were protonated. The spectrum of the chitosan coating, which was coated on alginate, showed the absorption peaks at 1584, 1075 and 1035 cm^{-1}, which were related to amine II, C–O stretching and O–H bending (Manjubala, Scheler, Bössert, & Jandt,

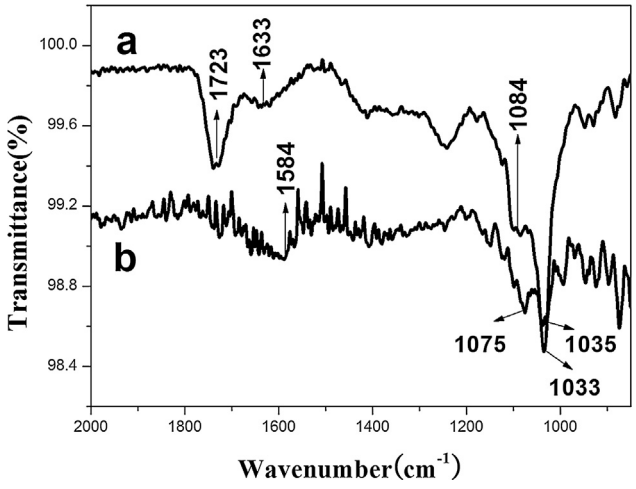

Fig. 2. ATR–FTIR spectra of alginate/chitosan coatings: (a) alginate coating; (b) chitosan coating.

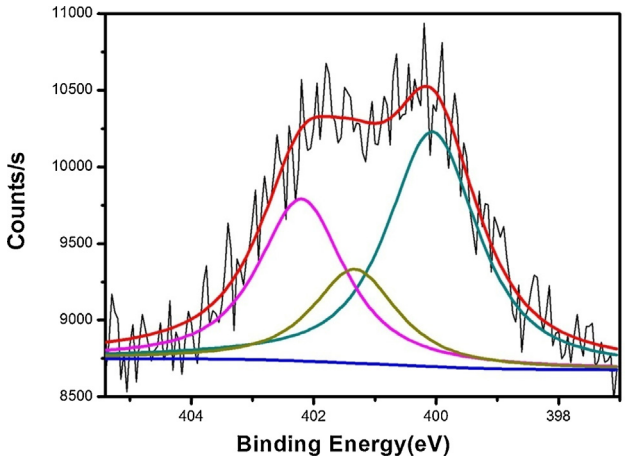

Fig. 3. XPS N 1s narrow scans with the curve fit of alginate/chitosan coatings cast from electrodeposition.

2006), respectively. The ATR–FTIR results proved that alginate and chitosan could deposite on the titanium substrate and form layer-by-layer structure by electrodeposition.

3.3. XPS spectra of chitosan/alginate layer-by-layer coatings

XPS is capable of quantifying the extent of protonation of amine groups through examination of the N 1s narrow scan; however, it is difficult to obtain the degree of deprotonation of carboxylic acid groups. The XPS spectrum of alginate coating, obtained by electrodeposition of sodium alginate using methanoic acid, revealed almost no sodium but only carbon and oxygen (the results were not shown here). This indicated that carboxylate groups of were protonated, which agreed with the results of ATR–FTIR. XPS is a complementary technique yielding information about the atomic composition of a material's surface, about 10 nm scanning depth. It can only quantify the amount of elements of chitosan when measuring the alginate/chitosan coatings. As showed in Fig. 3, the N 1s peak required three peaks for the curve fit: at 400.1 eV (amine), at 401.3 eV (amide), at 402.2 eV (protonated amine). In the coatings, less than half of the amine groups were protonated (49.4 atom % amine; 32.4 atom % protonated amine). The results showed that the chitosan coating contained protonated and deprotonated amine, thus chitosan coating and alginate coating could interact through static electricity and form chitosan/alginate layer-by-layer composite coatings on titanium substrates.

3.4. XRD analysis

To assess the interaction between two layers of chitosan/alginate, XRD was used and the results were shown in Fig. 4. The XRD patterns of chitosan power displayed two strong diffraction peaks at $2\theta = 10.4^\circ$, $2\theta = 21.8^\circ$, indicating the high degree of crystallinity of chitosan, their crystal lattice constant α corresponding to 8.470 and 4.075 (Qi, Xu, Jiang, Hu, & Zou, 2004). With the thickness of alginate coating increased, the peak at $2\theta = 21.8^\circ$ became much broader, which was attributed to the hydrogen bonding between amino groups and hydroxyl groups in the chitosan was broken by complexation (Kim & Lee, 1993). The results were related to the electrostatic interaction between chitosan and alginate. The XRD patterns indicated that chitosan in all coatings was predominantly in amorphous form, which was in accord with previous reports, who found that the chitosan in composite coatings prepared via electrodeposition also in amorphous form (Cheong & Zhitomisrky, 2008).

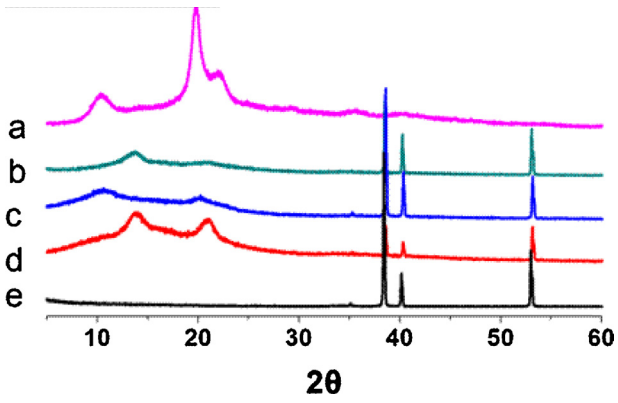

Fig. 4. XRD patterns of pure chitosan and alginate/chitosan coatings: (a) chitosan power; (b) alginate/chitosan; (c) alginate/chitosan/alginate; (d) pure chitosan coating; and (e) titanium.

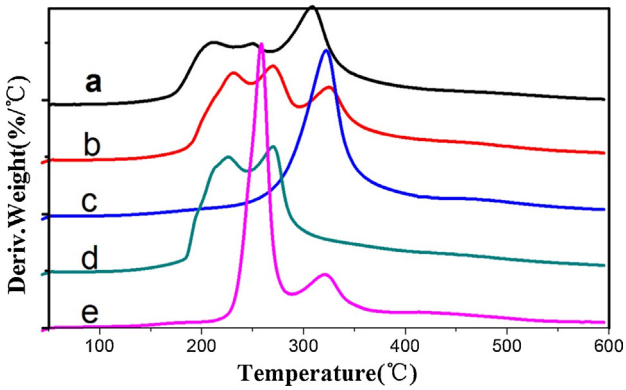

Fig. 5. DTG curves of (a) alginate/chitosan coatings; (b) alginate/chitosan/alginate coatings; (c) chitosan coating; (d) alginate coating, (e) sodium alginate/chitosan physical mixture (sodium alginate: chitosan mass ratio of 3:1).

3.5. Thermal analysis

Fig. 5 showed DTA data for the composite coatings, including alginate coating, chitosan coating, sodium alginate/chitosan physical mixture (sodium alginate:chitosan mass ratio of 3:1), alginate/chitosan coatings and alginate/chitosan/alginate coatings, respectively. As it is known, polysaccharides had a strong

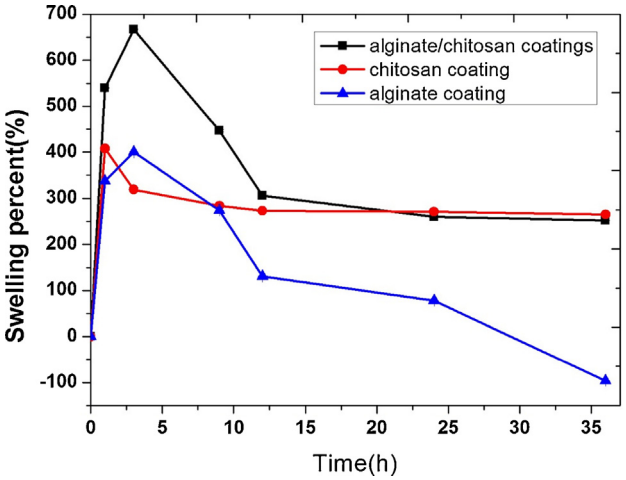

Fig. 6. Swelling degree of chitosan coating, alginate coating and alginate/chitosan coatings.

affinity for water and their hydration properties depend on their primary and supramolecular structures (Despond, Espuche, Cartier, & Domard2005). For all polymers, the first stage started below 150 °C to remove most of water. The second stage of polymers degradation corresponded to the thermal decomposition of pure polyelectrolytes or layer-by-layer complexes coatings and vaporization and elimination of volatile products. For chitosan coating the second stage started at 200 °C and reached a maximum at 308 °C, but for alginate coating it started at 190 °C and reached one maximum at 214 °C and the second one at 258 °C. Alginate/chitosan mixture revealed two stages (three peaks) of fast thermal degradation at 255 °C and 317 °C, which have some difference with characteristic for both components coatings. Thermogram of alginate/chitosan composite coatings was different from those of pure polymers and their mixture. The peak at about 250 °C typical for pure sodium alginate was not observed and the peak of pure chitosan had some changes. The results indicated that the interaction between alginate and chitosan coatings and might be considered as a proof of their complexation. Fig. 5(a) showed DTA data for the alginate/chitosan composite coatings. The alginate content in the composite coatings was about 20% degradation and chitosan was about 39.4% degradation. As shown in Fig. 5(b), the alginate/chitosan/alginate layer-by-layer composite coatings have the similar degradation temperature with alginate/chitosan coatings. What's more, the alginate content was about 34.9% degradation and chitosan was about 32.7% degradation. The results were in agreement with the electrodeposition of layers of alginate and chitosan.

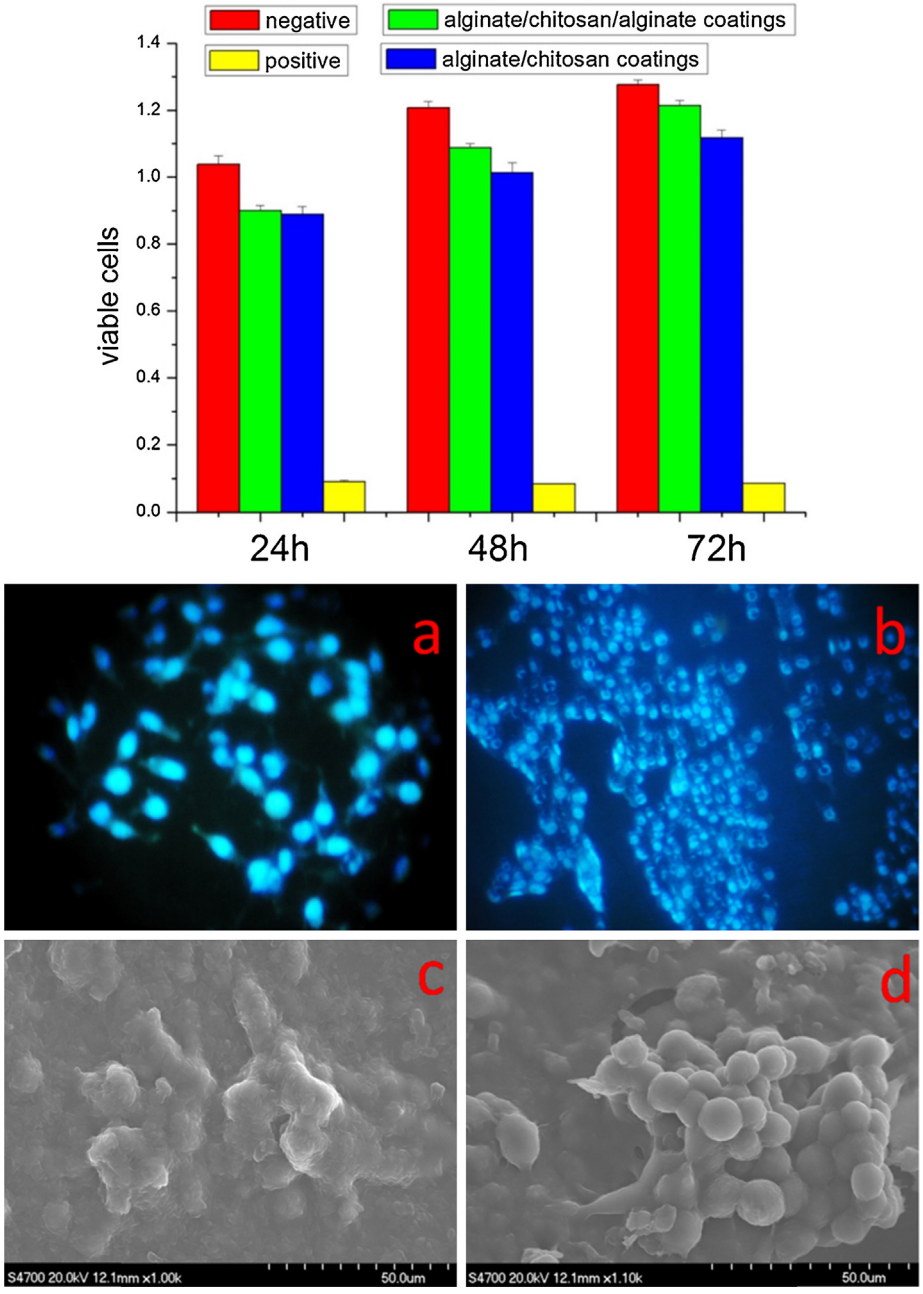

Fig. 7. Evaluation of the cellular activity after 24 h, 48 h and 72 h.; Cell fluorescence images of (a) alginate/chitosan coatings, and (b) alginate/chitosan/alginate coatings; SEM micrographs of cell morphology on (c) alginate/chitosan coatings, and (d) alginate/chitosan/alginate coatings.

3.6. Swelling properties study

The swelling properties of chitosan coating, alginate coating and alginate/chitosan coatings were shown in Fig. 6. It illustrated the changes in swelling percent of coatings with prolonged time. In the beginning, each coating showed a higher swelling degree and reached the maximum about 3 h. After 3 h, the swelling percentage of alginate coating and alginate/chitosan coatings decreased quickly, while chitosan coating showed minor changes. After 12 h, the swelling percentage of chitosan coating and alginate/chitosan coatings became constant, while alginate coating continued to decrease until 36 h. The results showed that each electrodeposited coating had strong ability of water uptake after the coating swelled in buffer solution. The alginate molecules could form partial network structure by physical crosslinking in the process of electrodeposition, so the alginate coating absorbed much water, but then dissolved in buffer gradually for the break of physical crosslinking. For chitosan coating, there were abundant hydroxyl and amino groups between chitosan molecules and they could form strong hydrogen bond. Thus, the chitosan coating absorbed water, but could not be dissolved. The swelling degree of chitosan coating decreased and then became constant, which was related with the fact that electrodeposition process might circumvent any impurities and the chitosan coating contained protonated chitosan and deprotonated chitosan, and deprotonated chitosan dissolved in the solution. The results were in accordance with XPS results. The phenomenon that at 12 h, the swelling degree of alginate/chitosan coating was larger than chitosan coating could be attributed to the formation of composite polyelectrolyte between chitosan layer and alginate layer through electrostatic interaction and the composite polyelectrolyte had a certain thickness to absorb water. After 12 h, the swelling percent of alginate/chitosan coating decreased less and became constant until 36 h. During this period of time, alginate layer in the alginate/chitosan coating continued to dissolve within a narrow range.

3.7. Cell cytotoxicity studies

The cytotoxicity of the materials was characterized by a MTT assay. The results showed that the coatings had higher cell viability than the positive control. A statistically significant difference between negative control and cells exposed to the coatings was observed, including 24 h, 48 h and 72 h of incubation, respectively. As shown in Fig. 7, there was almost no difference between alginate/chitosan coatings and alginate/chitosan/alginate coatings in 24 h of incubation. While after 48 h of incubation, there were more viable cells on the alginate/chitosan/alginate coatings than alginate/chitosan coatings. The results showed that the alginate/chitosan/alginate coatings were more suitable for cells proliferation.

The cytocompatibility of coatings was further characterized through in vitro studies. Cell fluorescence images and SEM analysis (Fig. 7) were used to characterize cell adhesion and proliferation. In situ observation of cells and coatings revealed that only a few cells located on the alginate/chitosan coatings, as shown in Fig. 7(c). One possible reason is the strong electrostatic interaction between the negative charges of the surface of cell membranes and the cationic sites on the chains of chitosan, which restricted cell spreading and proliferation (Mao et al., 2004). In vitro cytocompatibility tests showed that alginate/chitosan/alginate coatings achieved better cell response, as shown in Fig. 7(d). The results were in accord with some other articles report that alginate gels are promising for cell transplantation in tissue engineering and have favorable properties, including biocompatibility and ease of gelation (Lee & Mooney, 2012).

4. Conclusions

In this paper, chitosan/alginate layer-by-layer composite coatings were prepared on titanium substrates via electrodeposition. It was found that the thickness of the deposited chitosan layer and alginate was about 20 μm and 10 μm, respectively. Just as anticipated, a new IR band appeared at 1723 cm^{-1}, revealing that the carboxylate groups of Na-alginate was protonated and Na-alginate solution could, under electrodeposited process, undergo a sol–gel transition, deposite on titanium substrates. XPS N1 narrow scans results proved that partial deprotonated chitosan and protonated chitosan were coelectrodeposited on titanium substrates, in accordance with ATR–FTIR results. The XRD results showed that electrostatic interaction existed between chitosan coating and alginate coating. In vitro biological tests showed that cell morphology showed good condition on the alginate/chitosan/alginate coatings as compared to alginate/chitosan coatings. The possibility of electrodeposition of alginate/chitosan layer-by-layer coatings provides opportunities in the fabrication of functional coatings on titanium substrates.

Acknowledgment

We gratefully acknowledge the financial support from National Natural Science Foundation of China (Grant No. 201304005) and Jiangsu Provincial Natural Science Foundation (Grant No. BK20131145).

References

Boccaccini, A. R., Keim, S., Ma, R., Li, Y., & Zhitomirsky, I. (2010). Electrophoretic deposition of biomaterials. *Journal of the Royal Society Interface*, *7*(Suppl 5), S581–S613.

Bumgardner, J. D., Wiser, R., Elder, S. H., Jouett, R., Yang, Y., & Ong, J. L. (2003). Contact angle, protein adsorption and osteoblast precursor cell attachment to chitosan coatings bonded to titanium. *Journal of Biomaterials Science, Polymer Edition*, *14*(12), 1401–1409.

Cai, K., Rechtenbach, A., Hao, J., Bossert, J., & Jandt, K. D. (2005). Polysaccharide-protein surface modification of titanium via a layer-by-layer technique: Characterization and cell behaviour aspects. *Biomaterials*, *26*(30), 5960–5971.

Cheng, Y., Luo, X., Betz, J., Buckhout-White, S., Bekdash, O., Payne, G. F., Bentley, W. E., & Rubloff, G. W. (2010). In situ quantitative visualization and characterization of chitosan electrodeposition with paired sidewall electrodes. *Soft Matter*, *6*(14), 3177.

Cheng, Y., Luo, X., Betz, J., Payne, G. F., Bentley, W. E., & Rubloff, G. W. (2011). Mechanism of anodic electrodeposition of calcium alginate. *Soft Matter*, *7*(12), 5677.

Cheong, M., & Zhitomirsky, I. (2008). Electrodeposition of alginic acid and composite films. *Colloids and Surfaces A: Physicochemical and Engineering Aspects*, *328*(1–3), 73–78.

Despond, S., Espuche, E., Cartier, N., & Domard, A. (2005). Hydration mechanism of polysaccharides: A comparative study. *Journal of Polymer Science Part B: Polymer Physics*, *43*(1), 48–58.

Fernandes, R., Wu, L.-Q., Chen, T., Yi, H., Rubloff, G. W., Ghodssi, R., Bentley, W. E., & Payne, G. F. (2003). Electrochemically induced deposition of a polysaccharide hydrogel onto a patterned surface. *Langmuir*, *19*(10), 4058–4062.

Glenis, S., Horowitz, G., Tourillon, G., & Garnier, F. (1984). Electrochemically grown polythiophene and poly(3-methylthiophene) organic photovoltaic cells. *Thin Solid Films*, *111*(2), 93–103.

Gray, K. M., Liba, B. D., Wang, Y., Cheng, Y., Rubloff, G. W., Bentley, W. E., Montembault, A., Royaud, I., David, L., & Payne, G. F. (2012). Electrodeposition of a biopolymeric hydrogel: Potential for one-step protein electroaddressing. *Biomacromolecules*, *13*(4), 1181–1189.

Kim, J. H., & Lee, Y. M. (1993). Synthesis and properties of diethylaminoethyl chitosan. *Polymer*, *34*(9), 1952–1957.

López-Lacomba, J. L., García-Cantalejo, J. M., Sanz Casado, J. V., Abarrategi, A., Correas Magaña, V., & Ramos, V. (2006). Use of rhBMP-2 activated chitosan films to improve osseointegration. *Biomacromolecules*, *7*(3), 792–798.

Lawrie, G., Keen, I., Drew, B., Chandler-Temple, A., Rintoul, L., Fredericks, P., & Grøndahl, L. (2007). Interactions between alginate and chitosan biopolymers characterized using FTIR and XPS. *Biomacromolecules*, *8*(8), 2533–2541.

Lee, K. Y., & Mooney, D. J. (2012). Alginate: Properties and biomedical applications. *Progress in Polymrer Science*, *37*(1), 106–126.

Luo, X. L., Xu, J. J., Du, Y., & Chen, H. Y. (2004). A glucose biosensor based on chitosan-glucose oxidase-gold nanoparticles biocomposite formed by one-step electrodeposition. *Analytical Biochemistry*, *334*(2), 284–289.

Manjubala, I., Scheler, S., Bössert, J., & Jandt, K. D. (2006). Mineralisation of chitosan scaffolds with nano-apatite formation by double diffusion technique. *Acta Biomaterialia*, *2*(1), 75–84.

Mao, J. S., Cui, Y. L., Wang, X. H., Sun, Y., Yin, Y. J., Zhao, H. M., & De Yao, K. (2004). A preliminary study on chitosan and gelatin polyelectrolyte complex cytocompatibility by cell cycle and apoptosis analysis. *Biomaterials*, *25*(18), 3973–3981.

Qi, L., Xu, Z., Jiang, X., Hu, C., & Zou, X. (2004). Preparation and antibacterial activity of chitosan nanoparticles. *Carbohydrate Research*, *339*(16), 2693–2700.

Redepenning, J., Venkataraman, G., Chen, J., & Stafford, N. (2003). Electrochemical preparation of chitosan/hydroxyapatite composite coatings on titanium substrates. *Journal of Biomedical Materials Research Part A*, *66A*(2), 411–416.

Roether, J. A., Boccaccini, A. R., Hench, L. L., Maquet, V., Gautier, S., & Jérôme, R. (2002). Development and in vitro characterisation of novel bioresorbable and bioactive composite materials based on polylactide foams and bioglass® for tissue engineering applications. *Biomaterials*, *23*(18), 3871–3878.

Sartori, C., Finch, D. S., Ralph, B., & Gilding, K. (1997). Determination of the cation content of alginate thin films by FTIR spectroscopy. *Polymer*, *38*(1), 43–51.

Yang, C., Xu, L., Zhou, Y., Zhang, X., Huang, X., Wang, M., Han, Y., Zhai, M., Wei, S., & Li, J. (2010). A green fabrication approach of gelatin/CM-chitosan hybrid hydrogel for wound healing. *Carbohydrate Polymers*, *82*(4), 1297–1305.

Yin, Y. J., Yao, K. D., Cheng, G. X., & Ma, J. B. (1999). Properties of polyelectrolyte complex films of chitosan and gelatin. *Polymer International*, *48*(6), 429–432.

Zhitomirsky, D., Roether, J. A., Boccaccini, A. R., & Zhitomirsky, I. (2009). Electrophoretic deposition of bioactive glass/polymer composite coatings with and without HA nanoparticle inclusions for biomedical applications. *Journal of Materials Processing Technology*, *209*(4), 1853–1860.